

A Comparison study of Drag correlations for a Dispersed Multiphase flow in a Fluidized bed

Siva Karthikeya M¹, Ashley Melvin², Divyesh Variya³, Janani Sree Murallidharan⁴

¹Department of Aerospace Engineering, SASTRA Deemed University, Thanjavur-781039, India

²FOSSEE, IIT Bombay, Mumbai-400076, India

³Department of Mechanical Engineering, IIT Bombay, Mumbai-400076, India

ABSTRACT

The present study compares different drag models like Syamlal O'Brien, Gidaspow Ergun WenYu (GEW), and Gidaspow Schiller Naumann (GSN) in the modeling of fluidized-bed. With the help of the open-source CFD software OpenFOAM, time-averaged particle velocity components were calculated at five lateral locations of the fluidized bed. Later these values were used for validation against experimental data generated by the National Energy Technology Laboratory (NETL). Particles belonging to Geldart group D are considered as the particulate phase in this study, which is fluidized by gas at ambient conditions. The Eulerian-Eulerian approach is adopted for the present 2D computational study with closures from the Kinetic Theory of Granular Flow (KTGF). The study identified the Syamlal O'Brien drag closure to be reliable in modeling the interfacial momentum transfer phenomenon between the phases. Thus, it accurately predicted the particle velocity distribution at different lateral locations of the fluidized bed. It was also observed that the accuracy of the predictions made by Gidaspow Ergun WenYu (GEW) drag closure reduced significantly as the gas velocity increases at the domain inlet.

Keywords: OpenFOAM, CFD, Fluidized bed, Multiphase

1. INTRODUCTION

Research on sustainable technologies has burgeoned in the 21st century to tackle environmental degradation occurring at every stage of any industrial process. Fluidized bed technology is one such potential deployment into the category of sustainable technologies, widely used in the pharmaceutical, petroleum, chemical, and many other industries and has been at a focal point of research.

With the primary function of making a solid-fluid mixture behave as a fluid, this technology has the potential to reduce the harmful gas emissions from industries without compromising on the efficiency of results like combustion, catalytic cracking, and other chemical processes. For further advancement and proliferation of this technology, research into Computational models that are capable of predicting the flow structure inside the Fluidized Bed accurately is of key interest. This study analyses the reliability of various drag correlations in modeling the interfacial momentum transfer between the existing phases in a Fluidized bed phenomenon.

2. LITERATURE REVIEW AND OBJECTIVE

Systematic validation and uncertainty quantification of CFD models for Multiphase flows have been the fundamental objective of the small-scale challenge put forth by NETL in 2013 [1]. As a part of this challenge, the experimental data obtained by measuring the pressure drop and the particle velocities at various locations of a rectangular bed were made available to the research community for validation purposes. A low frequency (1 Hz) and a high frequency (1kHz) pressure transducers are used to extract the pressure drop data. Parallely, High-speed Particle Image Velocimetry is used to obtain the particle velocity at the desired locations [2]. Present research involves validating the CFD results obtained for three drag correlations against the experimental data to quantify the uncertainties of each drag closure. Considering the interfacial momentum transfer phenomena between the phases in a Multiphase flow simulation is essential in obtaining accurate results. Neglecting this can lead to an introduction of relative errors as large as 30% into the normally obtained results [3]. Hence, it is important to investigate the factors that contribute to the momentum transfer between phases in a Multiphase Flow. A detailed formulation of these factors is provided in Enwald et al. (1996) [4]. In the case of a solid-fluid dispersed flow, the generalized drag force term in the Reynolds averaged momentum equation predominantly contributes to the interfacial momentum transfer, unlike separated flows; where factors like interfacial pressure difference and combined interfacial shear plays a major role. Thus, evaluating the drag correlations available in the literature to model the Fluidized bed phenomenon has been a crucial aspect of the present research. Although multiple pieces of literature discussed various drag closures that can be implemented in OpenFOAM, studies [4] and [5] provided a comprehensive overview of the physics behind each drag closure and its operating phase fraction ranges. Considering the possibility of a drastic variation in phase fraction values at the interface of both the phases, the drag closures were chosen such that their operating ranges can accommodate both low and high-phase fraction regimes. The original Syamlal O'Brien drag closure in OpenFOAM was tuned based on the value of minimum fluidization velocity obtained from the experiment [1]. This step ensures that the computationally modeled drag force accurately mimics the experimental drag force. Similarly, the value of the Specularity coefficient, which is indicative of the wall roughness, is adapted from Lungu et al. (2016) [6] for a

superficial gas velocity of 3.28 m/s. Eulerian – Eulerian approach is chosen for this study due to its relative computational inexpensiveness when compared to other approaches. The fluidized bed being a dispersed system, multi-fluid modeling is used where both phases are treated as interpenetrating continua.

3. MATERIALS AND METHODS

The geometry, dimensions, and boundaries of the 2D fluidized-bed used for this study are shown in fig. 1. The geometric data used from [1], fig. 1 shows the parts of a Fluidized bed. The lateral locations, where the particle velocities measured for comparison with the experimental data produced by the National Energy Technology Laboratory (NETL) is also shown. Crucial parameters considered in the study, like the superficial gas velocity at the inlet, the initial phase fraction of the dispersed phase (particles) is mentioned in table 1. An initial phase fraction of 0.58 means that 58% of the static bed is occupied with the dispersed phase (particles) and the remaining 42% with the continuous phase (liquid). An entire domain is discretized into 2806 quadrilateral elements. The twoPhaseEulerFoam solver from OpenFOAM software is used for running the simulations.

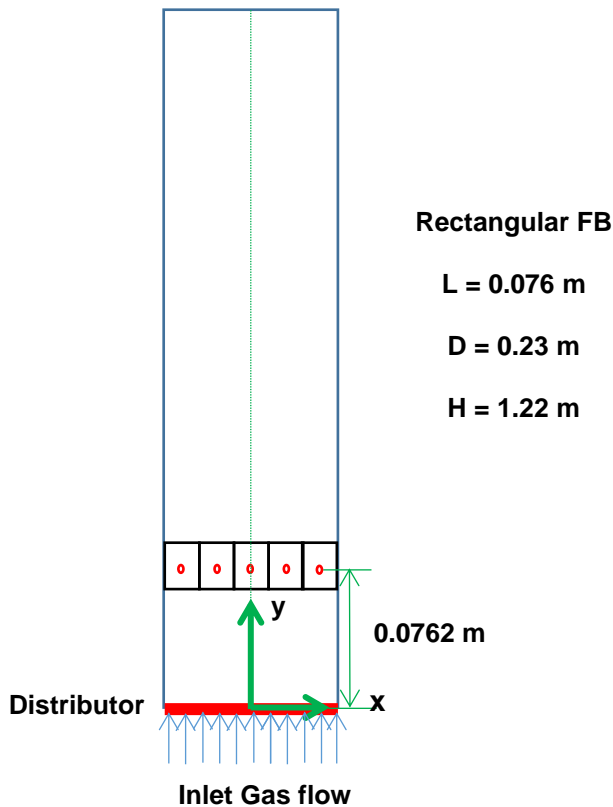


Figure 1: Schematic diagram of the set-up with dimensions [1]

Table 1: Parameters used in this study

Parameters	Value
Superficial Gas Velocities	2.19 m/s & 3.28 m/s
Minimum Fluidization Velocity	1.03 m/s
Static Bed Height	0.173 m
Initial phase fraction (α_i)	0.58
Gas density (ρ_g)	1.204 kg/m ³
Particle diameter (d_p)	3256 μ m
Particle density (ρ_p)	1131 kg/m ³
Specularity Coefficient (Φ)	0.125 & 0.05

3.1 Governing Equations

Multiphase flows can be numerically modeled using different approaches such as:

- Direct Numerical Simulation (DNS)
- Eulerian – Langrangian approach
- Eulerian – Eulerian approach

Eulerian – Eulerian approach is further classified based on the phase morphology into separated and dispersed systems [1]. For a dispersed system like the fluidized bed, multi-fluid modeling is used; where both phases are considered as interacting and interpenetrating continua, therefore, share the same continuity and momentum equations for each phase individually as shown in Eqs. (1), (2), and (4). For the solid phase, the Kinetic Theory of Granular Flow (KTGF) [7] was adopted for closure which considers the conservation of Solid Fluctuation Energy. KTGF approach is an extension to the classical kinetic theory of gases to dense granular flows, where the fluctuation energy is described using the granular temperature (θ).

Three important assumptions made in this study for simplification are:

- Both solid and liquid phases are isothermal.
- There is no interphase mass transfer between both phases.
- Solid particles are of pure spherical configuration with a mean diameter and density.

- Conservation of Mass ($k = f$ for fluid phase, s for solid phase)

$$\frac{\partial}{\partial t}(\alpha_k \rho_k) + \frac{\partial}{\partial x}(\alpha_k \rho_k \mathbf{u}_k) = 0 \quad (1)$$

- Conservation of Momentum (fluid phase)

$$\begin{aligned} \frac{\partial}{\partial t}(\alpha_f \rho_f \mathbf{u}_f) + \nabla \cdot (\alpha_f \rho_f \mathbf{u}_f \mathbf{u}_f) = \\ \alpha_f \nabla \cdot \bar{\boldsymbol{\tau}}_f + \alpha_f \rho_f \mathbf{g} - \alpha_f \nabla p - \mathbf{F}_{df} - \mathbf{F}_{vm} \\ - \mathbf{F}_{lf} \end{aligned} \quad (2)$$

$\mathbf{F}_{df}, \mathbf{F}_{lf}, \mathbf{F}_{vm}$ is the drag force, lift force, and virtual mass force respectively in Eqs. (2) and (4). Since drag force contributes predominantly to the momentum exchange between the fluid and particulate phases, it is given more importance in this study.

$$\bar{\boldsymbol{\tau}}_f = \mu_f \left[\nabla \mathbf{u}_f + (\nabla \mathbf{u}_f)^T \right] - \frac{2}{3} \mu_f (\nabla \cdot \mathbf{u}_f) \bar{\mathbf{I}} \quad (3)$$

The stress tensor of the liquid phase from Eq. (2) is expanded in Eq. (3) where μ_f is the combined turbulent and laminar viscosity for the fluid phase. Further, $k-\epsilon$ turbulence model is used in the study for the fluid phase.

- Conservation of Momentum (solid phase)

$$\begin{aligned} \frac{\partial}{\partial t}(\alpha_s \rho_s \mathbf{u}_s) + \nabla \cdot (\alpha_s \rho_s \mathbf{u}_s \mathbf{u}_s) = \\ -\alpha_s \nabla p - \nabla p_s + \nabla \cdot \bar{\boldsymbol{\tau}}_s + \alpha_s \rho_s \mathbf{g} + \mathbf{F}_{df} + \mathbf{F}_{vm} + \mathbf{F}_{lf} \end{aligned} \quad (4)$$

The solid phase stress tensor is expressed in terms of bulk solid viscosity ξ_s , and shear solid viscosity μ_s in Eq. (5)

- Conservation of Solid Fluctuation Energy

$$\begin{aligned} \frac{3}{2} \left[\frac{\partial}{\partial t}(\alpha_s \rho_s \theta) + \nabla \cdot (\alpha_s \rho_s \theta) \mathbf{u}_s \right] = \\ \left(-\nabla p_s \bar{\mathbf{I}} + \bar{\boldsymbol{\tau}}_s \right) : \nabla \mathbf{u}_s + \nabla \cdot (k_s \nabla \theta) - \gamma_s - 3\beta\theta + D_{l_s} \end{aligned} \quad (5)$$

Energy of fluctuating velocity of particle is measured using Granular temperature (θ)

3.2 Drag Correlations

Numerous drag correlations are available [1] that can model the mechanism of interfacial momentum transfer majorly caused due to drag force between the phases. A thorough literature study was performed to identify such drag correlations that could model the flow for all phase fraction regimes, individually or as a combination of two. It is necessary for a drag correlation to accurately predict the flow at all phase

fraction regimes. Because, the probability of a cell in a domain, especially at the interface, to overshoot the maximum phase fraction of the domain can never be neglected and must be taken into account. Also, the correlations adopted must be applicable for a multi-particle system to consider the effect of other particle's presence. Upon considering such fundamental factors, three drag correlations were chosen to model the two-phase flow inside a fluidized bed.

- Gidaspow Ergun WenYu:

It is a combination of the Ergun drag correlation applicable for dense systems and the Wen Yu correlation that can model a dilute flow where viscous forces are dominant, accurately.

This correlation uses the Ergun equation, Eq. (7), for $\alpha_p \geq 0.2$ and the Wen-Yu equation, Eq. (8) for $\alpha_p \leq 0.2$, where K is defined as the drag function for each correlation. Drag force in the Ergun correlation is calculated based on pressure drop per unit length, Eq. (9), unlike the Wen Yu correlation that considers the drag coefficient on a single particle, Eq. (10).

$$K = 150 \frac{\mu_g}{d_p} \frac{\alpha_p^2}{(1 - \alpha_p)^2} + 1.75 \frac{\rho_g U_r}{d_p} \frac{\alpha_p^2}{(1 - \alpha_p)^2} \quad (6)$$

$$K = \frac{3}{4d_p} C_{Ds} \alpha_p (1 - \alpha_p) \rho_g U_r (1 - \alpha_p)^{-2.65} \quad (7)$$

$$\frac{\Delta p}{L} = 150 \frac{\mu_g U_r}{d_p g} \frac{\alpha_p^2}{(1 - \alpha_p)^3} + 1.75 \frac{\rho_g U_r^2}{d_p g} \frac{\alpha_p}{(1 - \alpha_p)^3} \quad (8)$$

$$C_{Ds} = \begin{cases} \frac{24}{\text{Re}} (1 + 0.15 \text{Re}^{0.687}), & \text{Re} \leq 1000 \\ 0.44, & \text{Re} > 1000 \end{cases} \quad (9)$$

- Gidaspow Schiller Naumann:

This drag correlation is capable of calculating the drag in a multi-particle system, unlike the Schiller-Naumann correlation. Which is restricted to a single particle system only. The drag function for this correlation is defined in Eq. (11). Schiller-Naumann drag coefficient, Eq. (10), is used by replacing the Re with $(1 - \alpha_p)\text{Re}$, as shown in Eq. (12) below.

$$K = \frac{3}{4d_p} C_{Ds} \alpha_p (1 - \alpha_p) \rho_l U_r (1 - \alpha_p)^{-2.65} \quad (10)$$

$$C_{Ds} = \begin{cases} \frac{24}{(1 - \alpha_p)\text{Re}} (1 + 0.15 ((1 - \alpha_p)\text{Re})^{0.687}), & \text{Re} \leq 1000 \\ 0.44, & \text{Re} > 1000 \end{cases} \quad (11)$$

- Syamlal O'Brien

This drag correlation is based on the primary assumption that the Archimedes number remains the same for terminal

settling velocity for both single and multi-particle systems [7]. It uses the expression, Eq. (13), to relate the settling velocity and the void fraction, where Re_s is the Reynolds number for a single particle and V_r , the ratio of terminal settling velocity in a multi-particle system to that of a single particle system.

$$\frac{V_r - A}{B - V_r} = 0.06Re_s \quad (12)$$

$$V_r = 0.5(A - 0.06Re + \sqrt{(0.06Re)^2 + 0.12Re(2B - A) + A^2}) \quad (13)$$

$$A = (1 - \alpha_p)^{4.14} \quad (14)$$

$$B = \begin{cases} C_1(1 - \alpha_p)^{1.28}, & \alpha_p \geq 0.15 \\ (1 - \alpha_p)^{C_2}, & \alpha_p < 0.15 \end{cases} \quad (15)$$

Eq. (14), (15), and (16) are obtained by solving Eq. (13) after replacing Re_s with Re/V_r . Drag coefficient proposed by Dallavalle, Eq. (17), is used here to obtain the final drag function in Eq. (18), where \mathbf{U}_r is the relative interstitial velocity, $\mathbf{U}_g - \mathbf{U}_p$.

$$C_{Ds} = \left(0.63 + \frac{4.8}{\sqrt{Re_s}}\right)^2 \quad (16)$$

$$K = \frac{3\alpha_p(1 - \alpha_p)\rho_g}{4V_r^2 d_p} \left(0.63 + 4.8 \sqrt{\left(\frac{V_r}{Re}\right)}\right)^2 |\mathbf{U}_r| \quad (17)$$

The coefficients C_1 and C_2 in Eq. (16) are unique to a problem statement and depend on the parameters like Archimedes number, minimum fluidization velocity, and other physics properties of the individual phases. In our case, $C_1 = 0.88$ and $C_2 = 2.04$. Existing Syamlal O'Brien drag closure was tuned with the new coefficients by creating a new drag model with the name newSyamlalObrien.

3.3 Boundary Conditions

In a granular flow case, the particles neither stick to the wall nor slip freely on it. Thus, a wall boundary condition introduced by Johnson and Jackson [8] is implemented to the field variables of particles in the simulation. The boundary conditions are summarized in table 2 and 3.

Specularity coefficient (ϕ_s) is defined as the fraction of particle tangential momentum transferred to the wall through collisions. It is an indication of the wall roughness. This is affected by the superficial gas velocity and the particle size.

$(\phi_s) = 1 \Rightarrow$ Zero tangential velocity, maximum hindrance

$(\phi_s) = 0 \Rightarrow$ Free slip along the wall, minimum hindrance

In this study, the specularity coefficient was considered as 0.05 for 3.28 m/s gas velocity [5] and 0.125 for 2.19 m/s gas velocity which yielded more accurate results.

Table 2: Velocity boundary conditions considered in this study

Boundary	u_r (m/s)	u_s (m/s)
Inlet	2.19 and 3.28	Fixed Value
Outlet	Pressure Inlet Outlet	Fixed Value
Walls	noSlip	JohnsonJacksonParticleSlip

Table 3: Pressure boundary conditions considered in this study

Boundary	p_rgh
Inlet	fixedFluxPressure
Outlet	prghPressure
Walls	fixedFluxPressure

4. RESULTS AND DISCUSSION

Post-processing of the results was carried out in ParaView, open-source visualization software, and MS Excel. Particle velocity at different lateral locations was obtained by plotting the entire transient simulation over time for each lateral location to extract the velocity data at every time step for an overall time interval of 50 seconds. The extracted data was time-averaged in the time interval after a bubbling fluidization flow regime is established which is sustained till the end of the simulation. The results are then validated against the experimental data generated by National Energy Technology (NETL).

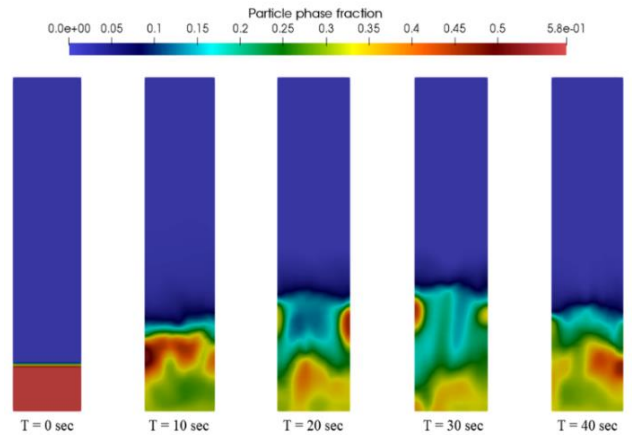


Figure 2: Contours of particle phase fraction (α_p) at five different timestamps

4.1 Case 1: Superficial Gas Velocity of 2.19 m/s

The time-averaged axial velocity data of the particles at different lateral locations of the fluidized bed is plotted in fig. 3 for various drag correlations. Experimental data generated by NETL for the same is included for comparison with the CFD results. Syamlal O'Brien drag closure is more accurate in predicting the axial particle velocity at all the lateral locations, followed by GEW. The trend of experimental results is followed by both Syamlal O'Brien and GEW but not GSN. The time-averaged axial velocity is the highest at the central location for all correlations except GSN.

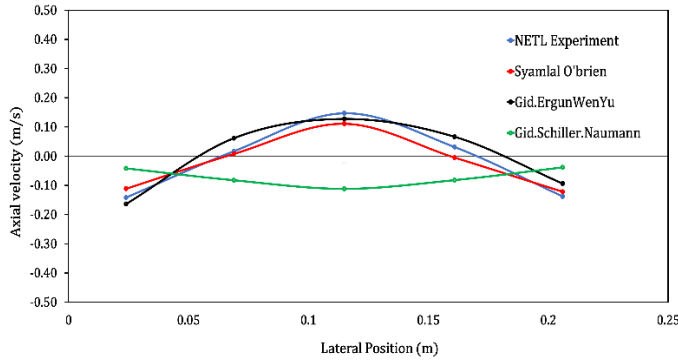


Figure 3: Axial velocity vs Lateral position plot for various drag correlations ($U_g = 2.19$ m/s).

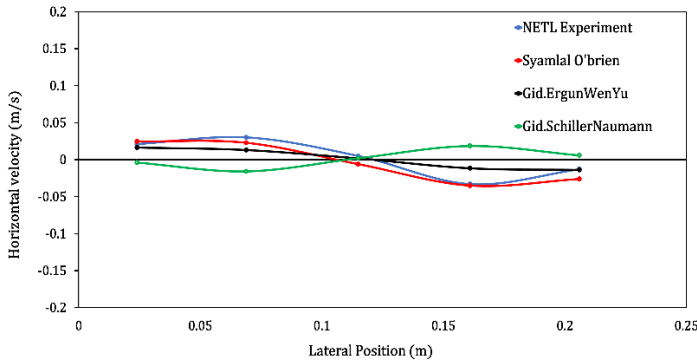


Figure 4: Horizontal velocity vs Lateral position plot for various drag correlations ($U_g = 2.19$ m/s).

The results obtained for horizontal velocity distribution, fig. 4, further, strengthen our inference made from the axial velocity results about the accuracy of the Syamlal O'Brien correlation because of its overlapping with the experimental results. However, the GEW closure is nearly as accurate as the Syamlal O'Brien closure for the first case. Similar to the axial velocity distribution, the GSN correlation fails to follow the trend of the experimental plot and overpredicts at most of the lateral positions.

4.2 Case 2: Superficial Gas Velocity of 3.28 m/s

Interesting behavior was observed in the axial velocity distribution when the superficial gas velocity was increased from 2.19 m/s to 3.28 m/s as shown in fig. 5. Syamlal O'Brien's closure again proved to be accurate among others. The direction of velocity at the five lateral locations for both GEW and Syamlal O'Brien closure

happens to be the same as that of experimental observations which is not the case with GSN. Though GEW closure has managed to successfully follow the trend of experimental results, it overpredicts the axial velocity at the center of the bed. The deviations observed in GSN closure have significantly increased from case 1 to case 2.

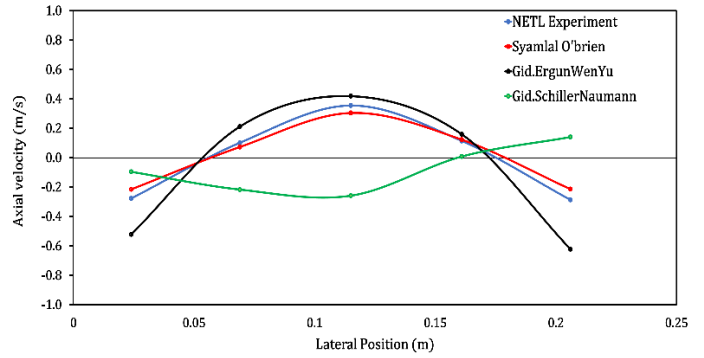


Figure 5: Axial velocity vs Lateral position plot for various drag correlations ($U_g = 3.28$ m/s).

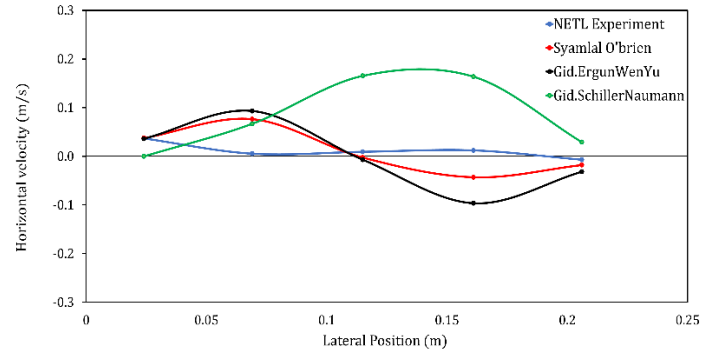


Figure 6: Horizontal velocity vs Lateral position plot for various drag correlations ($U_g = 3.28$ m/s).

The drag closures predict an opposite horizontal velocity trend from the experimental observations for case 2 as depicted in fig. 6. The experimentally obtained velocity profile also seems to reverse from that of case 1 due to the downward shift of the center of counter-rotating circulation cells [6].

The first significant inference to be drawn from the results is about the GSN closure that predicted the particle velocity distributions poorly for both the cases of gas velocity. Despite being developed to account for the particle-particle interactions by including the voidage function [4], it was the least accurate for both the velocity cases. It can be attributed to the fact that it was primarily developed for packed bed applications where the gas velocity is relatively low, restricting the flow regime to a fixed bed. The increase in relative error as the gas velocity is raised from 2.19 m/s to 3.28 m/s for the GSN closure reinforces our inference about the better performance of the model at low fluid velocities and dilute particle concentrations.

At first, a noble deviation was observed in the axial velocity plots at the central location for different drag closures when compared with the experimental counterpart. Changing the

specularity coefficient from 0.5 to 0.125 for cases 1 and 0.5 to 0.05 for case 2 provided the required bump in the axial velocity at the central location was observed for both GEW and Syamlal O'Brien drag correlations. Low values of specularity coefficient produce high particle velocities in the bed due to less loss of tangential momentum to the walls [5].

Finally, Syamlal O'Brien's drag correlation was most accurate in replicating the experimental results for both cases. The reason for this realistic behavior could be because of the consideration of the clustering effect [9] of particles in the model, unlike other correlations. GEW drag correlation performed on par with the Syamlal O'Brien model at lower gas velocity. As the gas velocity increases to 3.28 m/s, the trend in the horizontal and axial velocities was replicated exactly, a higher relative error than that of the Syamlal model makes it unsuitable at higher velocities.

5. CONCLUSIONS

This study was performed to identify the most reliable drag correlation for computational modeling of dispersed multiphase flows in a fluidized bed. The CFD results of particle velocity profiles obtained for different drag correlations were compared against the experimental data generated by NETL. Syamlal O'Brien drag correlation outperformed others for both the cases of superficial gas velocity, 2.19 m/s and 3.28 m/s, by accurately predicting the mean eulerian particle velocity distributions at various lateral locations of the fluidized bed. The Gidaspow Ergun WenYu correlation's predictions were on par with the former for the lower gas velocity of 2.19 m/s but are only satisfactory for the 3.28 m/s gas velocity case. The Gidaspow Schiller Naumann correlation was least accurate among the three in predicting the velocity profile but has given valuable insights about the model and its operating range.

ACKNOWLEDGEMENTS

The authors would like to thank the FOSSEE project, IIT Bombay for its financial support of this research. The authors also thank other members of our team, Mr. Ashley Melvin, and Ms. Swetha for their valuable inputs during discussions.

NOMENCLATURE

u	Velocity	[m/s]
F_{df}	Drag Force	[kg/m ² -s ²]
F_{lf}	Lift Force	[kg/m ² -s ²]
F_{vm}	Virtual Mass Force	[kg/m ² -s ²]
α	Phase fraction	--
ρ	Density	[kg/m ³]
C_D	Drag coefficient	--
μ	Dynamic Viscosity	[kg/m-s]
θ	Granular Temperature	[kg/m-s ²]
K	Drag Function	--
Φ	Specularity Coefficient	--
Re	Reynolds Number	--
V_r	Terminal Settling Velocity ratio	--

REFERENCES

- [1] National Energy Technology Laboratory (NETL). (2013, May 30). Small Scale Challenge Problem I (2013). <https://mfix.netl.doe.gov/experimentation/challenge-problems/small-scale-challenge-problem-i-2013/>
- [2] Balaji Gopalan, Mehrdad Shahn timer, Rupen Panday, Jonathan Tucker, Frank Shaffer, Lawrence Shadle, Joseph Mei, William Rogers, Chris Guenther, Madhava Syamlal, Measurements of pressure drop and particle velocity in a pseudo-2D rectangular bed with Geldart Group D particles, Powder Technology (2015), doi: 10.1016/j.powtec.2015.12.040
- [3] Bentsen, R. G. (1998). Effect of momentum transfer between fluid phases on effective mobility. Journal of Petroleum Science and Engineering, 21(1-2), 27–42. doi:10.1016/s0920-4105(98)00035-7
- [4] H, Enwald, E. Peirano, A-E Almstedt 'Eulerian Two-Phase Flow Theory Applied to Fluidization' Int. J. Multiphase Flow, Vol. 22, Suppl, pp. 21-66, 1996
- [5] Upadhyay, M., Kim, A., Kim, H., Lim, D., & Lim, H. (2020). An Assessment of Drag Models in Eulerian–Eulerian CFD Simulation of Gas–Solid Flow Hydrodynamics in Circulating Fluidized Bed Riser. ChemEngineering,4(2),37. doi:10.3390/chemengineering402003
- [6] Lungu, M., Wang, H., Wang, J., Yang, Y., & Chen, F. Two-Fluid Model Simulations of the National Energy Technology Laboratory Bubbling Fluidized Bed Challenge Problem. Industrial & Engineering Chemistry Research, 55(17), 5063–5077, 2016
- [7] Ding, J. and Gidaspow, D. A bubbling fluidization model using kinetic theory of granular flow. AIChE Journal 36, 523-538, 1990
- [8] Johnson, P. C., & Jackson, R. Frictional–collisional constitutive relations for granular materials, with application to plane shearing. Journal of Fluid Mechanics, 176(-1), 67, 1987
- [9] O'Brien, T. J. and Syamlal, M. Particle cluster effects in the numerical simulation of a circulating fluidized bed. 4th Int. Conf. on CFB, Somerset, USA, Preprint Volume, pp. 430—435, 199